Ca^{2+}–calmodulin-dependent myosin light chain kinase is essential for activation of TRPC5 channels expressed in HEK293 cells

Shunichi Shimizu[1], Takashi Yoshida[2], Minoru Wakamori[3,4], Masakazu Ishii[1,2], Takaharu Okada[3], Masami Takahashi[5], Minoru Seto[6], Katsuhiko Sakurada[6], Yuji Kiuchi[1] and Yasuo Mori[2,3]

[1] *Department of Pathophysiology, School of Pharmaceutical Sciences, Showa University, Tokyo 142-8555, Japan*
[2] *Center for Integrative Bioscience and* [3] *Department of Information Physiology, National Institute for Physiological Sciences, Okazaki, Aichi 444-8585, Japan*
[4] *Department of Physiology, Kagoshima University Faculty of Medicine, Kagoshima, Kagoshima 890-8520, Japan*
[5] *Mitsubishi Kagaku Institute of Life Sciences, Machida, Tokyo 194-8511, Japan*
[6] *Institute for Life Science Research, Asahi Kasei Corporation, Fuji, Shizuoka 416-0934, Japan*

Mammalian homologues of *Drosophila* transient receptor potential (TRP) proteins are responsible for receptor-activated Ca^{2+} influx in vertebrate cells. We previously reported the involvement of intracellular Ca^{2+} in the receptor-mediated activation of mammalian canonical transient receptor potential 5 (TRPC5) channels. Here we investigated the role of calmodulin, an important sensor of changes in intracellular Ca^{2+}, and its downstream cascades in the activation of recombinant TRPC5 channels in human embryonic kidney (HEK) 293 cells. Ca^{2+} entry through TRPC5 channels, induced upon stimulation of the G-protein-coupled ATP receptor, was abolished by treatment with W-13, an inhibitor of calmodulin. ML-9 and wortmannin, inhibitors of Ca^{2+}–calmodulin-dependent myosin light chain kinase (MLCK), and the expression of a dominant-negative mutant of MLCK inhibited the TRPC5 channel activity, revealing an essential role of MLCK in maintaining TRPC5 channel activity. It is important to note that ML-9 impaired the plasma membrane localization of TRPC5 channels. Furthermore, TRPC5 channel activity measured using the whole-cell patch-clamp technique was inhibited by ML-9, whereas TRPC5 channel activity observed in the cell-excised, inside-out patch was unaffected by ML-9. An antibody that recognizes phosphorylated myosin light chain (MLC) revealed that the basal level of phosphorylated MLC under unstimulated conditions was reduced by ML-9 in HEK293 cells. These findings strongly suggest that intracellular Ca^{2+}–calmodulin constitutively activates MLCK, thereby maintaining TRPC5 channel activity through the promotion of plasma membrane TRPC5 channel distribution under the control of phosphorylation/dephosphorylation equilibrium of MLC.

(Resubmitted 5 September 2005; accepted after revision 9 November 2005; first published online 10 November 2005)
Corresponding author S. Shimizu: Department of Pathophysiology, School of Pharmaceutical Sciences, Showa University, 1-5-8 Hatanodai, Shinagawa-ku, Tokyo 142-8555, Japan. Email: shun@pharm.showa-u.ac.jp

Changes in intracellular Ca^{2+} concentration ($[Ca^{2+}]_i$) play a vital role in the regulation of diverse cellular processes, including cell growth, cell differentiation, neurotransmitter release and muscle contraction (Clapham, 1995). In various types of cells, stimulation by agonists that activate phospholipase C (PLC) leads to a biphasic increase in $[Ca^{2+}]_i$. The first phase reflects Ca^{2+} release from intracellular Ca^{2+} stores (the endoplasmic reticulum) induced by inositol 1,4,5-trisphosphate (IP_3), while the sustained phase is due to the influx of Ca^{2+} from the extracellular space (Berridge, 1993; Bootman & Berridge, 1995; Clapham, 1995). At least two major classes of Ca^{2+}-permeable channels are involved in mediating the receptor-activated Ca^{2+} influx. The store-operated channel is activated by the depletion of intracellular Ca^{2+} stores following Ca^{2+} release (Putney, 1990; Fasolato *et al.* 1994; Berridge, 1995; Clapham, 1995). Activation of the other Ca^{2+}-permeable cation channels involves second messengers, but is independent of store depletion.

An important clue for understanding the molecular basis of receptor-activated Ca^{2+} influx was first obtained through the finding of a *Drosophila* visual transduction mutant, transient receptor potential (*trp*), whose photoreceptors fail to generate the Ca^{2+}-dependent sustained

 DOI: 10.1113/jphysiol.2005.097998

phase of receptor potential and to induce subsequent Ca^{2+}-dependent adaptation to light (Fein *et al.* 1984; Ranganathan *et al.* 1995). With regard to vertebrate TRP homologues, so far seven TRPC proteins have been reported (Petersen *et al.* 1995; Wes *et al.* 1995; Birnbaumer *et al.* 1996; Zhu *et al.* 1996; Philipp *et al.* 1998; Okada *et al.* 1998, 1999). Functional expression of human TRPC1 or TRPC3, bovine TRPC4 or mouse TRPC5, TRPC6 or TRPC7 channels in African green monkey kidney (COS), Chinese hamster ovary or human embryonic kidney (HEK) 293 cells results in the enhancement of either agonist- or thapsigargin-stimulated Ca^{2+} entry (Birnbaumer *et al.* 1996; Zhu *et al.* 1996, 1998; Philipp *et al.* 1996, 1998; Xu *et al.* 1997; Boulay *et al.* 1997; Okada *et al.* 1998, 1999). It has been shown that TRPC1 channels are activated by intracellular Ca^{2+}-store depletion (Zitt *et al.* 1996), and TRPC3 is also likely to be stimulated, at least in part, by intracellular Ca^{2+}-store depletion (Zitt *et al.* 1997; Zhu *et al.* 1998), whereas TRPC5, TRPC6 and TRPC7 channels are distinguishable from store-operated Ca^{2+} channels (Boulay *et al.* 1997; Okada *et al.* 1998, 1999).

Although the heterologously expressed TRPC channels have been shown to be activated by various factors, including the G-proteins $G\alpha_{11}$ and $G\alpha_q$ (Obukhov *et al.* 1996; Schaefer *et al.* 2000), IP_3 receptors (Kanki *et al.* 2001) and diacylglycerol (Hofmann *et al.* 1999), the exact mechanisms for the activation and regulation of TRPC channels are still largely unknown. Recent studies have shown that the activation of TRPC channels is regulated by an exocytosis-like mechanism (Cayouette *et al.* 2004; Bezzerides *et al.* 2004). Cayouette *et al.* (2004) described that the insertion of TRPC6 channels into the plasma membrane with an exocytotic mechanism by stimulation with G_q-protein-coupled receptor activation. Bezzerides *et al.* (2004) showed that growth factor initiates the rapid translocation of TRPC5 channels from vesicles just under the plasma membrane to the cell surface through the phosphatidylinositide 3-kinase pathway. Thus, the translocation of functional TRPC channels into the plasma membrane seems to be a crucial mechanism for their regulation of the function of TRPC channels.

Some reports show that TRPC channels are regulated by Ca^{2+}–calmodulin (Trost *et al.* 2001; Zhang *et al.* 2001; Boulay, 2002; Singh *et al.* 2002). Calmodulin is one of the most important sensors of intracellular Ca^{2+} changes (Klee & Vanaman, 1982). Boulay (2002) showed that calmodulin binds to TRPC6, in a Ca^{2+}-dependent manner, and activates the channel activity. In addition, it has been shown that TRPC3 is activated by $[Ca^{2+}]_i$, as infusion of Ca^{2+} into the cell through the patch pipette increases TRPC3 currents (Zitt *et al.* 1997). The importance of $[Ca^{2+}]_i$ has also been described for TRPC5 channel activity (Okada *et al.* 1998; Strübing *et al.* 2001; Zeng *et al.* 2004). Ca^{2+}–calmodulin complex could associate not only with TRPC channels directly but also with other downstream kinases including myosin light chain kinase (MLCK). In fact, MLCK, activated by Ca^{2+}–calmodulin complex (Kamm & Stull, 2001), has been reported to regulate the activity of various ionic channels in native mammalian cells, including guinea-pig gastric myocytes, rabbit portal vein myocytes and porcine aortic endothelial cells (Kim *et al.* 1997; Watanabe *et al.* 1998; Tran *et al.* 1999; Aromolaran *et al.* 2000). Watanabe *et al.* (1998) reported that MLCK plays an essential role in regulating the plasmalemmal Ca^{2+} influx induced by bradykinin, thapsigargin and fluid flow in porcine aortic endothelial cells. Kim *et al.* (1997) reported that ML-7, a chemical inhibitor of MLCK, inhibited the carbachol-activated non-selective cationic current in guinea-pig gastric myocytes. Moreover, Aromolaran *et al.* (2000) indicated that MLCK inhibitors blocked the non-selective cation current induced by noradrenaline, guanosine 5′-*O*-(3-thiotriphosphate) (GTPγS) or 1-oleoyl-2-acetyl-*sn*-glycerol. Thus, accumulating evidence supports the importance of MLCK in mediating the activation of various cation channels in native mammalian cells. However, the role of MLCK remains to be clarified in the activation of Ca^{2+}-permeable cation channels. In the present study, we investigated the involvement of Ca^{2+}–calmodulin-dependent cascades in the activation of recombinant TRPC5 channels, which we previously classified as the receptor-activated, store-independent Ca^{2+} channel (Okada *et al.* 1998). The present findings suggest that Ca^{2+}–calmodulin-activated MLCK is essential for maintaining the localization of activatable TRPC5 channels in the plasma membrane.

Methods

Identification of MLCK mRNA expression by reverse transcriptase-polymerase chain reaction

Total RNA was extracted from HEK293 cells by a modified guanidium isothiocyanate method using ISOGEN (Nippon Gene Co, Tokyo, Japan). Reverse transcription and PCR amplification from 0.5 μg total RNA were performed using rTth DNA polymerase (RT-PCR high plus, Toyobo Co, Osaka, Japan). The pairs of primers used for amplification of MLCK were 5′-CCAGGTGTCACTGATGCTAC-3′ and 5′-GCTGTGCACCTTCCTCTCTT (436 bp, brain/endothelial cell isoform, AC no. X85337 and U48959), 5′-GCGAAGCAGCTTGGTCAGCC-3′ and 5′-CTCCAGCTTGGACTCCCTTG-3′ (587 bp, brain/endothelial cell isoform, AC no. X85337 and U48959), and 5′-ACCTGGACCTCAAGCCAGAG-3′ and 5′-TGGGACTTAAGGCGTCGGTT-3′ (459 bp, skeletal muscle isoform, AC# AF325549). The thermocycler was programed to give an initial cycle consisting of reverse transcription for 30 min at 60°C and denaturation for 2 min at 94°C, followed

by 30 cycles of denaturation for 1 min at 94°C and annealing/extension for 1.5 min at 58°C. PCR products were electrophoresed on a 3% agarose (Agarose S, Wako Pure Chemical Co, Tokyo, Japan) gel containing ethidium bromide, and visualized by UV-induced fluorescence.

Molecular cloning of human MLCK

To isolate the human MLCK (hMLCK), three fragments were obtained by PCR amplification from a human whole-brain cDNA (Clontech) using the Marathon cDNA Amplification Kit (Clontech). The specific oligonucleotide primers used were as follows: hMLCK-P1 (5′-GTGGAGACGAGGCAGCCAACTGAG-3′) and hMLCK-P4 (5′-CTTCTCGATGGAGACGGAGCAGAG-3′) for hMLCK-A (nucleotide residues, 168–681); hMLCK-P5 (5′-AGCAGAAGCTGCAAGATGTTCATG-3′) and hMLCK-P8 (5′-AAAGTCCTCGTCAATGATGCGCTC-3′) for hMLCK-B (506–1869), or hMLCK-P9 (5′-AGAGAAAGAGAATATCCGGCAGGAG-3′) and hMLCK-11 (5′-GACTTAGAAACTGCTTTTCTCTGGC-3′) for hMLCK-C (1707–2977).

An expression plasmid for hMLCK was constructed as follows. A PCR product amplified from the clone hMLCK-A using a sense primer (5′-AAGAATTCCACCATGGATTTCCGCGCCAAC-3′) and hMLCK-P4, was digested with *Eco*RI and *Pfl*MI. hMLCK-B was digested with *Pfl*MI (593 and 1776). The other PCR product amplified from the clone hMLCK-C using hMLCK-P9 and an antisense primer (5′-GGTCTGTCGACTCACTCTTCTTCCTCTTCC-3′) was digested with *Pfl*MI and *Sal*I. The resulting fragments were ligated with the 5.5-kb *Eco*RI/*Sal*I fragment from pCI-neo (Promega) to yield pCI-neo-hMLCK. To yield a dominant-negative mutant of MLCK, deletion of a single amino acid residue (lysine 561; Klemke *et al.* 1997) was constructed using a sense primer (5′-GTCTGGGCAGGGTTCTTCAAGGCATATTC-3′) and an antisense primer (5′-GCCTTGAAGAACCCTGCCCAGACTTTTCG-3′). The clone of wild-type MLCK was confirmed by sequence analysis.

Mutation of potential MLCK sites

To substitute Ser698 in the TRPC5 channel sequence, sense primers T5-BaI(+) (5′-AGGTGGCACCTTACCACCTCCTTTC-3′) and T5-SA1(+) (5′-CAACTTGAGAGCCTTCACAGAACGTC-3′) were combined with antisense primers T5-SA1(−) (5′-GACGTTCTGTGAAGGCTCTCAAGTTG-3′) and T5-BaI(−) (5′-CCTTGGGCGCCACTAGCTCTTGGCACG-3′), respectively, and TRPC5 cDNA as a template for the first PCR amplification. To substitute Ser775, sense primers T5-BaI(+) (5′-AGGTGGCACCTTACCACCTCCTTTC-3′) and T5-SA2(+) (5′-GAAGCCTCTCCACCAGCGCTGCTGATTTCTCTCAAAGGGATGATAC-3′) were combined with antisense primers T5-SA2(−) (5′-CTTTGAGAGAAATCAGCAGCCTGGTGGAGAGGCTTCTTCTTGGATG-3′) and T5-BaI(−) (5′-CCTTGGGCGCCACTAGCTCTTGGCACG-3′), respectively, and TRPC5 cDNA for the first PCR amplification. To substitute Thr700, sense primers T5-BaI(+) (5′-AGGTGGCACCTTACCACCTCCTTTC-3′) and T5-TV(+) (5′- GAGAAGCTTCGTCGAACGTCATGCTGA-3′) were combined with antisense primers T5-TV(−) (5′-TCAGCATGACGTTCGACGAAGCTTCTC-3′) and T5-BaI(−) (5′-CCTTGGGCGCCACTAGCTCTTGGCACG-3′), respectively, and TRPC5 cDNA for the first PCR amplification. The pairs of resulting amplification products and the primers T5-BaI(+) and T5-BaI(−) were combined in the second PCR amplification. The resulting amplification products were digested with BanI to isolate the mutated fragments for replacement with the corresponding BanI(1964)/BanI(2466) fragment in the wild-type TRPC5 cDNA construct (Okada *et al.* 1998). The dominant-negative mutant of MLCK was confirmed by sequence analysis.

Recombinant expression in HEK293 cells

HEK293 cells were transfected with the recombinant plasmids pCI-neo-mTRPC5 plus πH3-CD8 containing the cDNA of the T-cell antigen CD8 (Jurman *et al.* 1994) as previously described (Okada *et al.* 1998). Transfection was carried out using SuperFect Transfection Reagent (QIAGEN, Hilden, Germany). Cells were trypsinized, diluted with Dulbecco's modified Eagle's medium (DMEM) containing 10% fetal bovine serum (FBS), 30 units ml^{-1} penicillin and 30 $\mu g\,ml^{-1}$ streptomycin, and plated onto glass coverslips precoated with poly D-lysine 18 h after transfection. Then, cells were subjected to measurements 36–66 h after plating on the coverslips. TRPC5 channel-expressing cells were selected through detection of CD8 coexpression using polystyrene microspheres precoated with antibody to CD8 (Dynabeads M-450 CD8; DYNAL, Oslo, Norway).

The plasmid pEGFP-N1-mTRPC5, which contains a cDNA sequence encoding the TRPC5 protein tagged at the C-terminus with enhanced green fluorescent protein (eGFP), was constructed as follows. The PCR technique was used to attach a *Bam*HI site at the 3′-terminal end of the protein-coding sequence of TRPC5 cDNA, and was digested with *Nar*I and *Bam*HI. The resulting *Nar*I (2469)-*Bam*HI fragment was ligated with the *Sal*I(vector)-*Nar*I (2469) fragment from pCI-neo-mTRPC5 (Okada *et al.* 1998) and the *Sal*I-*Bam*HI fragment from pEGFP-N1 (Clonetech) to yield pEGFP-N1-mTRP5.

Measurement of changes in $[Ca^{2+}]_i$

Cells on coverslips were loaded with fura-2 by incubation in DMEM containing 5 μM acetoxymethyl ester (AM) form of fura-2 and 10% FBS at 37°C for 30 min, and washed with the Hepes-buffered saline (HBS) containing (mM): NaCl 107, KCl 6, $MgSO_4$ 1.2, $CaCl_2$ 2, KH_2PO_4 1.2, glucose 11.5 and Hepes 20; adjusted to pH 7.4 with NaOH. The coverslips were then placed in a perfusion chamber mounted on the stage of the microscope. Fluorescence images of the cells were recorded and analysed with a video-image analysis system (ARGUS-20/CA, Hamamatsu Photonics, Hamamatsu, Japan). The fura-2 fluorescence at an emission wavelength of 510 nm (bandwidth, 20 nm) was observed by exciting fura-2 alternatingly at 340 and 380 nm (bandwidth, 11 nm). The 340/380 nm ratio images were obtained on a pixel by pixel basis, and were converted to Ca^{2+} concentrations by *in vitro* calibration. The calibration procedure was performed according to the method of Ueda & Okada (1989). Stock solutions of ATP (in water), W-13 (in water), ML-9 (in dimethyl sulphoxide), and wortmannin (in dimethyl sulphoxide) were diluted to their final concentrations just before use in HBS or Ca^{2+}-free HBS containing (mM): NaCl 107, KCl 6, $MgSO_4$ 1.2, KH_2PO_4 1.2, EGTA 0.5, glucose 11.5 and Hepes-NaOH 20; adjusted to pH 7.4. The diluted solutions were applied to the cells by perfusion. The final concentration of the vehicle did not exceed 0.1%. The number of CD8-positive cells ranged from 2 to 15 in the field of view during each experiment. Data were accumulated under each condition from between three and eight experiments using cells prepared through three to eight transfections.

Electrophysiology

For electrophysiological measurements, coverslips with cells were placed in dishes containing the solutions. Cells prepared in this manner had a membrane capacitance of 21.3 ± 2.3 pF ($n = 25$). Currents from cells were recorded at room temperature using whole-cell patch-clamp techniques (Hamill *et al.* 1981) with an EPC-7 patch-clamp amplifier (List-Medical, Darmstadt, Germany) or Axopatch 200B patch-clamp amplifier (Axon Instruments, Union City, CA, USA). Patch pipettes were made from borosilicate glass capillaries (outer diameter, 1.5 mm; Hilgenberg, Malsfeld, Germany) using a model P-87 Flaming-Brown micropipette puller (Sutter Instrument, San Rafael, CA, USA). Pipette resistance ranged from 2 to 4 MΩ when filled with the pipette solution described below. Currents were sampled at 200 Hz for the conventional whole-cell mode, and at 2 kHz for the single-channel recording after low-pass filtering at 1 kHz. The pipette solution, for recordings of the whole-cell currents and the unitary currents using the whole-cell mode, contained (mM): CsOH 105, aspartic acid 105, CsCl 40, $MgCl_2$ 2, $CaCl_2$ 1.3, EGTA 5, Na_2ATP 2 and Hepes 5; adjusted to pH 7.2 with CsOH. The calculated free Ca^{2+} concentration was 50 nM. The '$0Ca^{2+}$' external solution contained (mM): NaCl 140, $MgCl_2$ 1.2, $CaCl_2$ 1.2, EGTA 10, glucose 10 and Hepes 11.5; adjusted to pH 7.4 with NaOH (calculated free $[Ca^{2+}]$, 8 nM). The bath solution for the inside-out recording contained (mM): CsCl 155, $CaCl_2$ 1.83, $MgCl_2$ 1, EGTA 2 and Hepes 5; adjusted to pH 7.3 with CsOH (calculated free $[Ca^{2+}]$, 1 μM). The pipette solution contained (mM): NaCl 122.4, $MgCl_2$ 1.2, $CaCl_2$ 2, ATP 0.1, glucose 30 and Hepes 11.5; adjusted to pH 7.4 with NaOH. Rapid exchange of the external solutions surrounding the cell was made within 300 ms by a modified 'Y-tube' method (Okada *et al.* 1998).

Biotinylation of cell surface protein

The cell surface TRPC5 was measured by biotinylation according to a modification of the method of Cayouette *et al.* (2004). Cells grown in 60-mm dishes were washed with HBS and treated with ML-9 (10 μM). After incubation for various periods (0–8 min), the cells were washed with ice-cold PBS containing (mM): NaCl 137, KCl 3.5, $CaCl_2$ 0.9, $MgCl_2$ 1 , NaH_2PO_4 10 (pH 7.4) and then incubated with Sulfo-NHS-SS-Biotin (Pierce) for 15 min at 4°C. The biotinylation reaction was stopped by the addition of 100 mM glycine, and the cells were washed with PBS twice to remove free biotin. The cells were then lysed with 1 ml ice-cold lysis buffer containing (mM): NaCl 150, EDTA 5 , phenylmethylsulphonyl fluoride 0.1 and Tris-HCl 20, with 1% Nonidet P40, 0.5% deoxycholate, 0.1% SDS, 1 μg ml^{-1} soybean trypsin inhibitor and 5 μg ml^{-1} leupeptin (pH 7.4), and sonicated for 5 s. After centrifugation, the supernatant was collected and incubated with streptoavidin-agarose beads (Pierce) overnight at 4°C. The samples were washed with lysis buffer three times and eluted by boiling for 5 min in × 2 Laemmli buffer before SDS-PAGE fractionation and Western blotting.

Western blot analysis

TRPC5-transfected HEK293 cells and non-transfected control HEK293 cells were lysed, and the obtained supernatants were subjected to SDS-polyacrylamide gels under reducing conditions. In short, proteins were transferred to a nitrocellulose membrane (Hybond ECL, Amersham Pharmacia Biotech, Buckinghamshire, UK) in buffer containing 150 mM glycine, 20 mM Tris-base and 10% (v/v) methanol at 600 mA, 4°C for 2 h. Non-specific binding was blocked with TBS plus 0.1% Tween 20 and blocking reagent (Western blotting analysis system, Amersham Pharmacia Biotech) for 40 min at room temperature. The blots were

incubated with a 1 : 200 dilution of anti-TRPC5 antibody, a 1 : 1000 dilution of antiglyceroaldehyde-3-phosphate dehydrogenase (GAPDH, Santa Cruz Biotechnology Inc., CA, USA) or a 1 : 50 dilution of antiphospho-myosin light chain (MLC) antibody that recognizes only mono-phosphorylated 20-kDa MLC at amino acid residue of (Ser^{19}) (Sakurada *et al.* 1998), for 50 min at room temperature. The blots were washed with TBS containing 0.1% Tween 20 for 30 min at room temperature. Antibodies retained on the blots were visualized using a Western blotting analysis system from Amersham Pharmacia Biotech.

Time-lapse image acquisition and analysis

The living cell image acquisition was performed at 25°C. Images were acquired using a confocal laser-scanning microscope (FV500, Olympus). Cells were observed with a 60 × Objective lens. eGFP fluorescence was excited with the 488-nm line of an argon laser. Emission light was filtered through a 505-nm long-pass filter. For data analysis, the entire cell was imaged under non-saturating conditions. Time-lapse image capturing and data evaluation were performed using the image analysis software, Fluoview (Olympus).

In Fig. 8*A*, fluorescence intensity was measured for selected areas of HEK293 cell. The fluorescence images were recorded at 30-s intervals.

Evanescent imaging of eGFP–TRPC5 fusion protein

The eGFP–TRPC5 fusion protein was visualized using an evanescent illumination system. E-GFP-F (Clontech) was used as the marker for plasma membrane localization. The incident light for evanescent illumination was introduced from the objective lens (CFI Plan Apo TIRF 100 ×; NA, 1.45; Nikon, Tokyo, Japan) installed on an inverted microscope (TE2000-U, Nikon). To observe the eGFP fluorescence image, a 488-nm laser (diode-pumped solid state, 20 mW; COHERENT, Inc., Santa Clara, CA, USA) for the evanescent wave excitation and a long-pass filter (515 nm) for the barrier were used. Fluorescence images were captured with a monochromatic cooled CCD camera (ORCA C4742-95, Hamamatsu Photonics, Hamamatsu, Japan). Total fluorescence was subtracted from background fluorescence. The video images were contrast-enhanced with a digital image processor (AQUACOSMOS, Hamamatsu Photonics), and finally stored on a computer hard disk.

For quantification, the total cellular fluorescence intensity was measured from each cell. The surface of the cell was outlined on screen using a mouse in order to determine the total cellular fluorescence intensity, which was calculated using the image analysis program AQUACOSMOS ver. 2.5. Total cellular fluorescence intensity was then expressed as a percentage of the resting (control, background-subtracted) fluorescence intensity. The mean percentage of total cellular fluorescence intensity was determined.

Statistical analysis

Results are presented as means ± S.E.M. of n observations. Each experiment was performed at least three times to confirm reproducibility of the obtained data. The statistical significance of observed differences was determined by analysis of variance followed by Tukey's test. Differences among means were considered significant when P was less than 0.05.

Results

Implication of Ca^{2+}–calmodulin and its downstream MLCK in TRPC5 channel-mediated Ca^{2+} entry

We previously showed that free Ca^{2+} in the intrapipette solution is required for the activation of TRPC5 ionic currents in patch-clamp recordings, suggesting that Ca^{2+} is essential for the activation of TRPC5 channels (Okada *et al.* 1998). Calmodulin is one of the most important sensors of changes in $[Ca^{2+}]_i$ (Klee & Vanaman, 1982). To determine whether calmodulin is required to activate TRPC5 channels, we first examined the effect of the calmodulin antagonist W-13 on the activation of TRPC5 channels by ATP-receptor stimulation (Fig. 1*A* and *B*). A protocol designed to separate the $[Ca^{2+}]_i$ rise by Ca^{2+} influx from that by Ca^{2+} release from the intracellular Ca^{2+} store was employed as previously described (Okada *et al.* 1998). ATP was first applied in the absence of extracellular Ca^{2+}, and 2 mM Ca^{2+} was added to the extracellular solution when $[Ca^{2+}]_i$ returned to the basal level (2 min after addition of ATP). The ATP-induced $[Ca^{2+}]_i$ transients in the absence of extracellular Ca^{2+} in TRPC5-transfected cells were not different from the vector-transfected control cells (data not shown; Okada *et al.* 1998). Re-addition of Ca^{2+} to the extracellular solution only slightly raised $[Ca^{2+}]_i$ to near the resting level in control cells (data not shown; Okada *et al.* 1998), whereas in TRPC5-transfected cells, it elicited dramatic $[Ca^{2+}]_i$ rise (Fig. 1*A*, *C* and *E*; Okada *et al.* 1998). Treatment with W-13 effectively inhibited this $[Ca^{2+}]_i$ rise by the addition of extracellular Ca^{2+} in ATP-stimulated TRPC5-transfected HEK293 cells in a dose-dependent manner. Chlorpromazine is also an inhibitor of calmodulin (Gillette & Green, 1983). Pretreatment with chlorpromazine (100 μM) for 30 min also reduced the ATP-induced Ca^{2+} entry through TRPC5 channels by 87.0 ± 9.2% ($n = 28$ for control and $n = 32$ for chlorpromazine; data not shown). These results suggest that calmodulin is involved in the activation of Ca^{2+} entry via TRPC5 channels.

MLCK is a target of Ca^{2+}–calmodulin (Kamm & Stull, 2001). We next studied the effects of MLCK inhibitors on the ATP-evoked Ca^{2+} influx in TRPC5-transfected HEK293 cells. ML-9, an inhibitor of MLCK, strongly and selectively inhibited $[Ca^{2+}]_i$ rises attributable to Ca^{2+} influx via TRPC5 channels (Fig. 1*C* and *D*). Wortmannin, another inhibitor of MLCK, also inhibited TRPC5-mediated $[Ca^{2+}]_i$ rises in a concentration-dependent manner (Fig. 1*E* and *F*). Wortmannin also is a weak inhibitor of phosphatidylinositol-3-kinase (PI3-kinase). However, pretreatment with a selective inhibitor of PI3-kinase LY294002 (25 μM) for 15 min, did not affect TRPC5-mediated Ca^{2+} influx (data not shown), suggesting that MLCK but not PI3-kinase plays a crucial role in the activation of TRPC5 channels.

To directly examine the ionic currents generated by TRPC5 channels, whole-cell patch-clamp recording was used. In vector-transfected cells, the current was unaffected by 100 μM ATP or 10 μM ML-9 at a holding potential of −60 mV (data not shown). However, the addition of ATP to the 2 mM Ca^{2+}-containing external solution evoked a rapid development of inward currents in TRPC5-transfected HEK293 cells (Fig. 2*A*). Decay

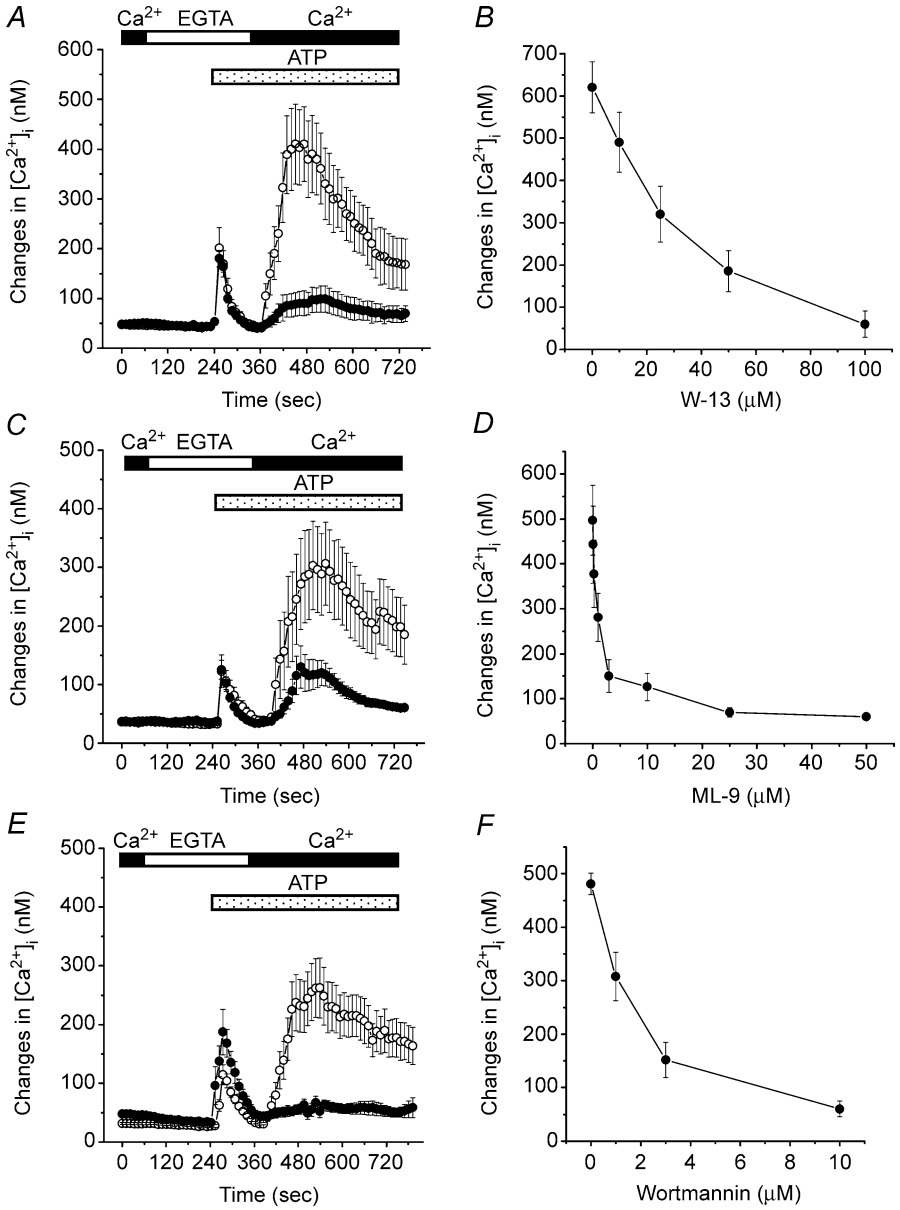

Figure 1. Effects of inhibitors of calmodulin and MLCK on TRPC5-mediated $[Ca^{2+}]_i$ rise in HEK293 cells
The fura-2-loaded HEK293 cells transfected with TRPC5 plus CD8 were incubated with (●) or without (○) various inhibitors. Cells were pretreated with W-13 (*A*, 100 μM) for 30 min ($n = 37$ cells for control and $n = 22$ for W-13 treatment), ML-9 (*C*, 3 μM) for 5 min ($n = 23$ for control and $n = 22$ for ML-9 treatment) or wortmannin (*E*, 10 μM) for 30 min ($n = 40$ for control and $n = 25$ for wortmannin treatment), and then cytosolic $[Ca^{2+}]_i$ was measured. The perfusion solution was first changed to Ca^{2+}-free HBS (shown as EGTA). Two minutes after the endogenous ATP receptor was stimulated by application of 100 μM ATP to the cells in the absence of extracellular Ca^{2+}, 2 mM Ca^{2+} was applied to induce rises in $[Ca^{2+}]_i$ due to Ca^{2+} entry via TRPC5 channels. All inhibitors were present throughout the time of Ca^{2+} measurement. The amplitude of maximum $[Ca^{2+}]_i$ rises induced by Ca^{2+} entry via TRPC5 channels in individual cells was plotted against various concentrations of W-13 (*B*), ML-9 (*D*) and wortmannin (*F*). The concentration of blocker that reduced the response to 50% of the control value (IC_{50}) was determined using Origin Version 6 J (OriginLab Corp, Northampton, MA, USA). IC_{50} values were 32.15, 0.72 and 1.43 μM for W-13, ML-9 and Wortmannin, respectively. Data points are the means ± S.E.M. of 13–45 cells for three to six experiments.

of the ATP-induced TRPC5 current was significantly accelerated by the replacement of extracellular 2 mM Ca^{2+} by 2 mM Ba^{2+} (Fig. 2*B*). We next examined the effects of inhibitors of calmodulin and MLCK on the ATP-induced inward current. The inward current was markedly inhibited by the extracellular application of 100 μM W-13 (Fig. 2*C*), 10 μM ML-9 (Fig. 2*D*), or 10 μM wortmannin (Fig. 2*E*), and the inhibitory effects of theses drugs on the peak current are summarized in Fig. 2*F*. Moreover, the inhibitory effect of ML-9 on the ATP-induced inward current through TRPC5 channels was reversible (Fig. 2*G*). Thus, in the activation of TRPC5 currents induced by ATP-receptor stimulation, electrophysiological measurements confirm the important involvement of Ca^{2+}–calmodulin-dependent MLCK revealed through pharmacological experiments.

Previously, we demonstrated that recombinant TRPC5 channels elicit low but significant basal activity, which can be characterized at unitary levels using the conventional whole-cell patch-clamp technique in a low Ca^{2+}-containing external solution (Yamada *et al.* 2000). Extracellular application of the MLCK inhibitor ML-9 (10 μM) significantly diminished the basal unitary TRPC5 channel activity, nP_o (n is the number of the channel, and P_o is the open probability; Fig. 3*A* and *B*). The TRPC5 channel activity recovered from the inhibition by ML-9 after washout (Fig. 3*B*). Under the conditions we employed, vector-transfected control cells failed to show spontaneous unitary activity (Yamada *et al.* 2000) or response to ML-9. By contrast, the application of ML-9 (10 mM) the intracellular side failed to affect TRPC5 channel activity in the excised plasma membrane patch using the inside-out mode of the patch-clamp technique (Fig. 3*C* and *D*). These results strongly suggest that ML-9 blocks TRPC5 channel activity through the inhibition of cytosolic enzyme MLCK, but not through direct action on the TRPC5 channels.

Endogenous MLCK expression and MLC phosphorylation in HEK293 cells

Expression of MLCK mRNA in HEK293 cells was identified using the RT-PCR method (Fig. 4*A*). When specific primers for brain/endothelial cell (EC) type MLCK were used, the bands that represented brain/EC-type MLCK were detected, suggesting that brain/EC-type MLCK is expressed in HEK293 cells. In contrast, the expression of skeletal muscle-type MLCK was not detected.

We next investigated the changes in the level of mono-phosphorylated MLC by treatment with ATP and ML-9 using an antiphospho-MLC antibody in HEK293 cells. We found, unexpectedly, that the addition of 100 μM ATP did not increase the level of monophosphorylated MLC (Fig. 4*B*). However, 10 μM ML-9 decreased the level of monophosphorylated MLC in a time-dependent manner (Fig. 4*C*). The application of 100 μM ATP after pretreatment with 10 μM ML-9 resulted in low levels of monophosphorylated MLC (Fig. 4*D*). Moreover, to examine the role of intracellular Ca^{2+} on phospho-MLC levels, the effect of the cell-permeable Ca^{2+} chelator BAPTA-AM was investigated. The treatment with BAPTA-AM (10 μM) decreased the basal levels of intracellular Ca^{2+} (data not shown), and the levels of phospho-MLC were also reduced by treatment with BAPTA-AM (Fig. 4*E*). These results provide evidence that MLC expressed in HEK293 cells is constitutively phosphorylated by MLCK in the presence of basal level of $Ca^{2+}{}_i$.

Inhibitory effect of the dominant-negative MLCK mutant on TRPC5-mediated Ca^{2+} influx

To directly examine the role of MLCK on the activation of TRPC5-mediated Ca^{2+} influx, the wild-type MLCK or the dominant-negative mutant MLCK were co-expressed with TRPC5 channels, and the ATP-induced $[Ca^{2+}]_i$ rise was compared with that in cells expressing TRPC5 alone (Fig. 5*A* and *B*). Deletion of a single amino acid residue (Lys^{561}) was introduced in MLCK (Mut-MLCK) to create the dominant-negative form of MLCK, as reported previously (Klemke *et al.* 1997). Co-expression of the dominant-negative mutant of MLCK strongly reduced the ATP-induced $Ca^{2+}{}_i$ entry through TRPC5 channels. However, TRPC5-mediated $[Ca^{2+}]_i$ rises were not significantly affected by the co-expression of wild-type MLCK. Moreover, TRPC5 expression was unaffected by the cotransfection of Mut-MLCK. These observations support the assumption that MLCK plays an important role in TRPC5 channel activation.

Intact Ca^{2+} influx activity of TRPC5 constructs with mutations at putative phosphorylation sites for MLCK in TRPC5 channels

According to the reported consensus sequence for MLCK phosphorylation, three candidate Ser/Thr amino acid residues, Ser^{698} (S698), Ser^{775} (S775), and Thr^{700} (T700) may be important in the TRPC5 sequence (Kemp *et al.* 1987; Nairn & Picciotto, 1994). To test the possibility that direct phosphorylation of the TRPC5 protein is responsible for the activation of TRPC5 induced by ATP-receptor stimulation, S698, S775 and T700 were mutated to Ala, Ala and Val, respectively (single mutants, S698A, S775A and T700V; a double mutant, S698A·S775A; and a triple mutant, S698A·S775A·T700V), and the ATP-evoked $[Ca^{2+}]_i$ rise and ionic currents generated by wild-type TRPC5 and mutated TRPC5 channels were measured. The increases in $[Ca^{2+}]_i$

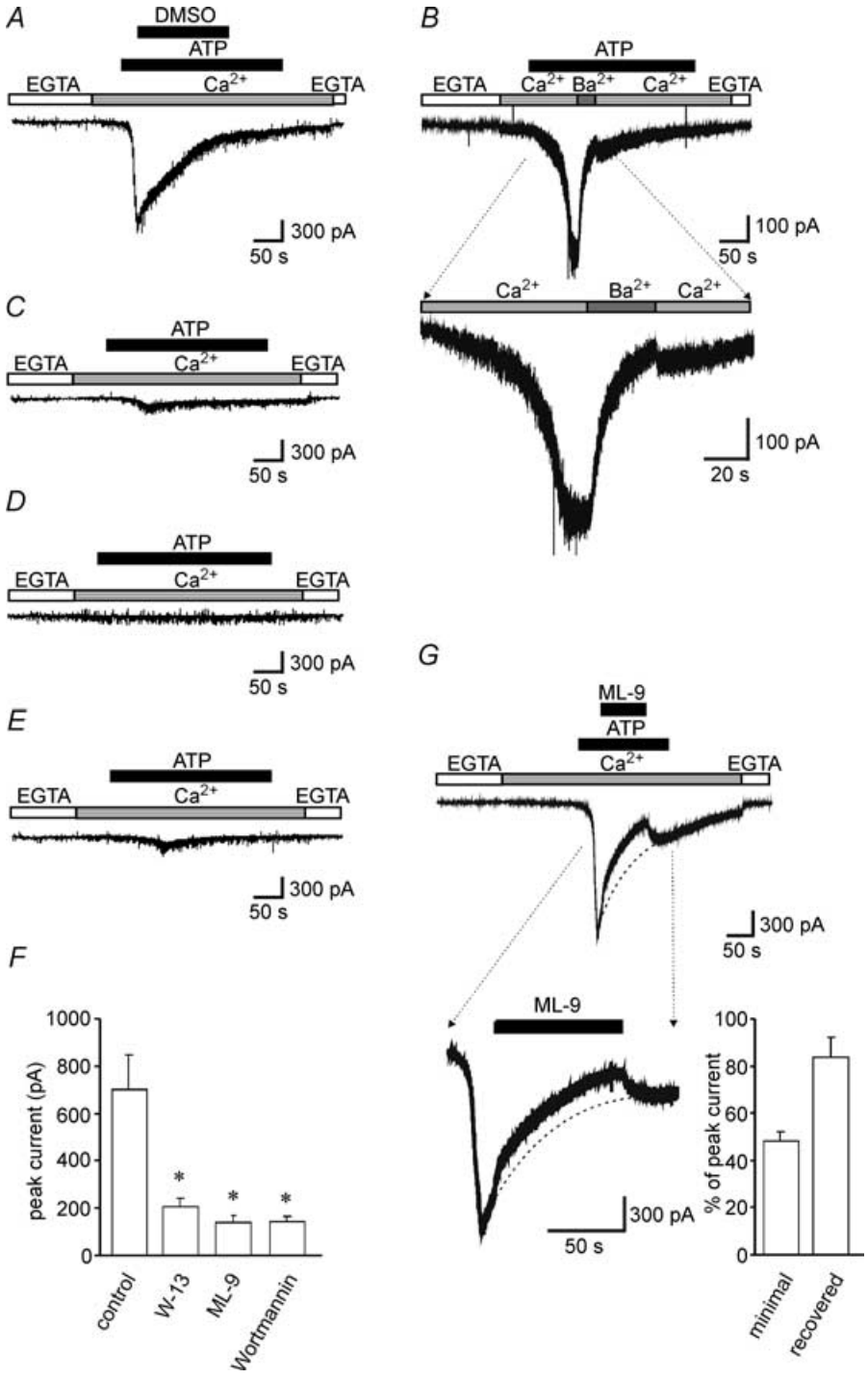

Figure 2. Effects of inhibitors of Ca^{2+}–calmodulin pathway on the ATP-induced TRPC5 channel activity
Ionic current was recorded from a HEK293 cell transfected with TRPC5 plus CD8 at a holding potential of −60 mV. *A*, the perfusion solution was first changed from Ca^{2+}-free solution (shown as EGTA) to 2 mM Ca^{2+}-containing solution, and 100 μM ATP was applied. Dimethyl sulphoxide (3.3 mM) used as solvent for the drugs failed to affect TRPC5 currents. *B*, the perfusion solution was first changed from Ca^{2+}-free solution to 2 mM Ca^{2+}-containing solution, and 100 μM ATP was applied. Ba^{2+} (2 mM) was applied to the cells after currents induced by ATP reached maximum levels. Cells were pretreated with 100 μM W-13 for 30 min (*C*), 10 μM ML-9 for 5 min (*D*) and 10 μM wortmannin for 30 min (*E*), and then the ATP-induced currents were measured using the same protocol as in *A*. All inhibitors were present throughout the period of Ca^{2+} measurement. *F*, the peak TRPC5 currents after inhibition by the drugs are summarized ($n = 37$, 25, 12 and 11 for control, W-13, ML-9 and wortmannin, respectively). $^*P < 0.05$ *versus* control group. *G*, the perfusion solution was first changed from Ca^{2+}-free solution

by the re-addition of extracellular Ca^{2+} following ATP-receptor stimulation in wild-type, S698A, S775A, T700V, S698A·S775A and S698A·S775A·T700V were 225.4 ± 41.3 nM, 164.6 ± 34.5 nM, 186.6 ± 37.6 nM, 171.7 ± 30.3 nM, 157.9 ± 35.2 nM and 169.3 ± 39.3 nM, respectively; however, these differences were not statistically significant. Moreover, the ATP-evoked inward current in the triple-mutant TRPC5 channel was unchanged compared with the wild-type TRPC5 channel (Fig. 6). Thus, the activation of TRPC5 channels was not significantly affected by any of the mutations of putative MLCK phosphorylation sites (Ser^{698}, Ser^{775} and Thr^{700}). This suggests that the ATP-receptor-induced activation of TRPC5 channels is independent of direct phosphorylation of TRPC5 by MLCK.

Role of MLCK in the plasma membrane distribution of TRPC5 channels

As MLCK is involved in cell motility and morphology, we used the biotinylation reaction to assess the possibility that MLCK controls the cell surface expression of TRPC5 channels. Treatment with ATP did not affect the surface expression of TRPC5 channels (Fig. 7*A*). However, ML-9 (10 μM) decreased surface TRPC5 levels time-dependently (Fig. 7*B*). These results suggest that the basal MLCK activity is crucial to maintaining the cell surface localization of TRPC5 channels.

To confirm the role of MLCK on the plasma membrane localization of TRPC5 channels, we observed the fluorescence of eGFP–TRPC5 expressed in a single HEK293 cell using a confocal microscope. Most TRPC5-GFP fluorescence was localized at the plasma membrane (Fig. 8*A*, left panel). After ML-9 treatment (10 μM), eGFP–TRPC5 was accumulated to form clusters near the plasma membrane (Fig. 8*A*, middle panel and inset), and was internalized to the cytosol (Fig. 8*A* right panel). The cytosolic fluorescence intensity was increased, accompanied with a loss of eGFP–TRPC5 from the plasma membrane (Fig. 8*B*).

To obtain further information about the translocation of TRPC5 channels at the plasma membrane, we used an evanescent wave microscope. Many fluorescent spots of a uniform size were distributed over the bottom area of the eGFP–TRPC5-expressed cell, in comparison with the uniform expression of the pEGFP-F (clontech), which remained bound to the plasma membrane (Fig. 8*C*). Treatment with ML-9 induced a marked decrease in the total intensity of fluorescence in only 60 s in the eGFP-TRPC5-expressing cell, whereas with dimethyl sulphoxide or ML-9 treatment of the pEGFP-F-expressing HEK293 cell, such fluorescence decrease was not observed (Fig. 8*C*, right panel). The decrease in intensity mainly reflected a loss of fluorescence from the evanescent field of eGFP–TRPC5 in the central portion of the plasma membrane facing the glass coverslip.

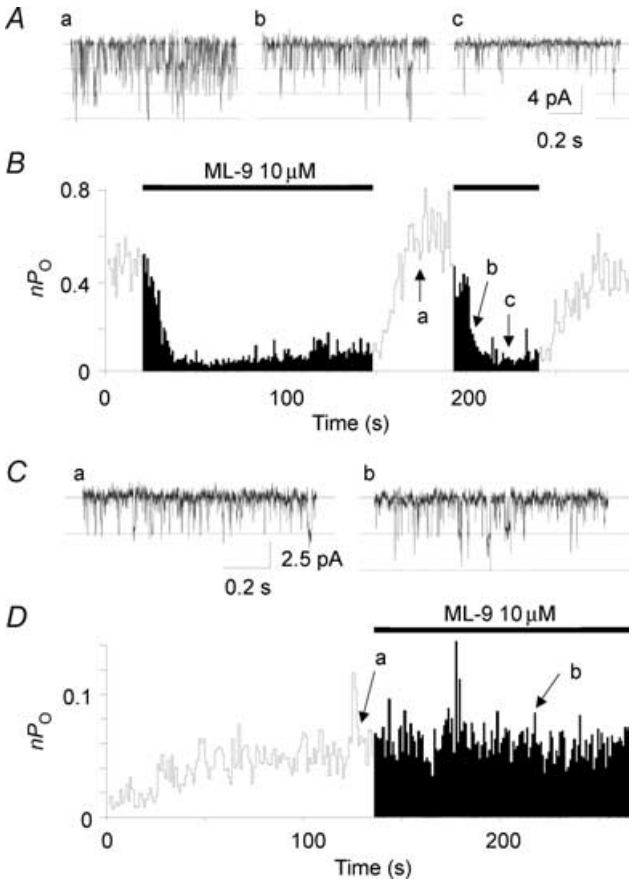

Figure 3. Inhibitory effect of ML-9 on TRPC5 channel is observed in whole-cell mode but not in cell-excised, inside-outside mode of patch-clamp recording
Traces of single-channel currents recorded by the whole-cell mode (*A*) or the inside-out mode (*C*) of the patch-clamp technique before (a) and during the application of 10 μM ML-9 (b and c) from the outside (A) or from the inside (C) of the membrane. A and C, a–c correspond to the time indicated by the arrows in *B* and *D*. Holding potential was −60 mV. The lines and the dotted lines indicate the closed and the open current levels. *B* and *D*, the plot of nP_o against time is shown. Values of nP_o are calculated every second. The bars indicate the duration of the exposure to 10 μM ML-9 from the outside (*B*) or from the inside (*D*) of the membrane. Similar results were obtained from four and six cells in the whole-cell and in the inside-out mode, respectively.

to 2 mM Ca^{2+}-containing solution, and 100 μM ATP was applied. During ATP treatment, 10 μM ML-9 was also added for 90 s (left panel). The right panel shows minimal ATP-induced TRPC5 currents during ML-9 treatment for 90 s (minimal,% peak ATP-induced TRPC5 currents before ML-9 application) and peak TRPC5 currents recovered after omission of ML-9 (recovered) ($n = 23$). The dashed line shows the typical declining current curve.

Discussion

Mammalian homologues of TRPC are molecular entities of receptor-activated Ca^{2+} channels. TRPC5 channels form a receptor-activated Ca^{2+} channel subtype, which is activated independently of Ca^{2+}-store depletion (Okada *et al.* 1998; Schaefer *et al.* 2000). However, the activation and the regulation mechanisms underlying G-protein-coupled receptor stimulation remain elusive. In the present study, we revealed the critical role of Ca^{2+}–calmodulin-dependent MLCK in the cell surface localization of activatable TRPC5 channels.

Implication of Ca^{2+}–calmodulin in the functional expression of TRPC5 channels

Cytosolic free Ca^{2+} has been shown to play an important role in the activation of TRPC5 channels (Okada *et al.* 1998; Strübing *et al.* 2001; Zeng *et al.* 2004). However, the pathways underlying this Ca^{2+}-dependent activation are yet to be elucidated for TRPC5 channels. An increase in $[Ca^{2+}]_i$ regulates various Ca^{2+}-binding proteins including calmodulin (Hanson & Schulman, 1992). Ca^{2+}–calmodulin complex directly or indirectly acts on various proteins. In the present study, ATP-induced

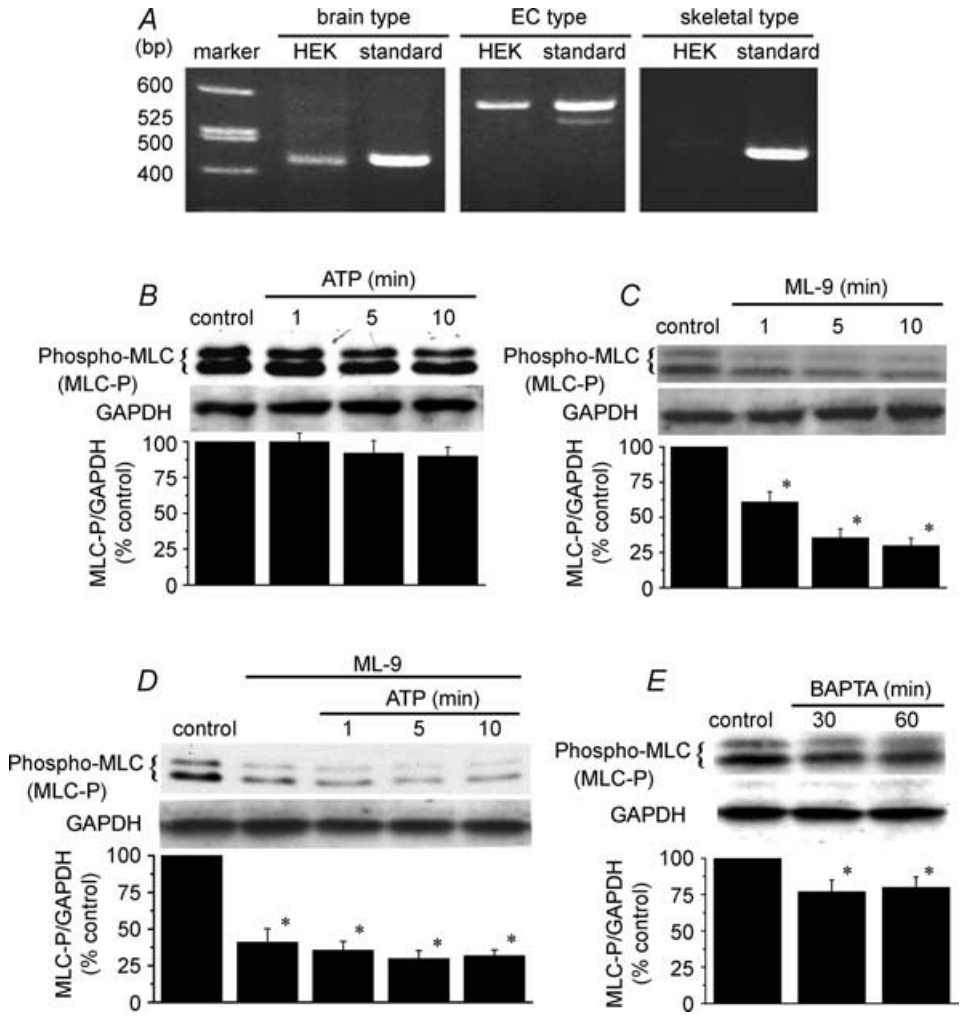

Figure 4. Endogenous expression of MLCK and reduction of phosphorylated levels of MLC by the MLCK inhibitor ML-9 in HEK293 cells

A, total RNA was extracted from HEK293 cells, and cDNA encoding the brain/EC-type MLCK (436 bp/587 bp) or the skeletal muscle-type MLCK (459 bp) was amplified by RT-PCR. Each right lane was the standard bands obtained from total RNA from human brain (OriGene Tech. Inc., Rockville, MA, USA) or human skeletal muscle (OriGene Tech. Inc.). *B*, the cells were exposed to 100 μM ATP for various periods. At the indicated time after the addition of ATP, the phosphorylated MLC was detected by Western blotting. *C*, the cells were treated with 10 μM ML-9 for various periods, and the phosphorylated MLC levels were determined. *D*, the cells were pretreated with 10 μM ML-9 for 10 min, and then treated with 100 μM ATP. *E*, the cells were treated with BAPTA-AM (10 μM) for 30 and 60 min. The lower columns in *B*–*E* show the ratio density of phosphorylated MLC/antiglyceroaldehyde-3-phosphate dehydrogenase (GAPDH) from three independent experiments. $^*P < 0.05$ *versus* control group.

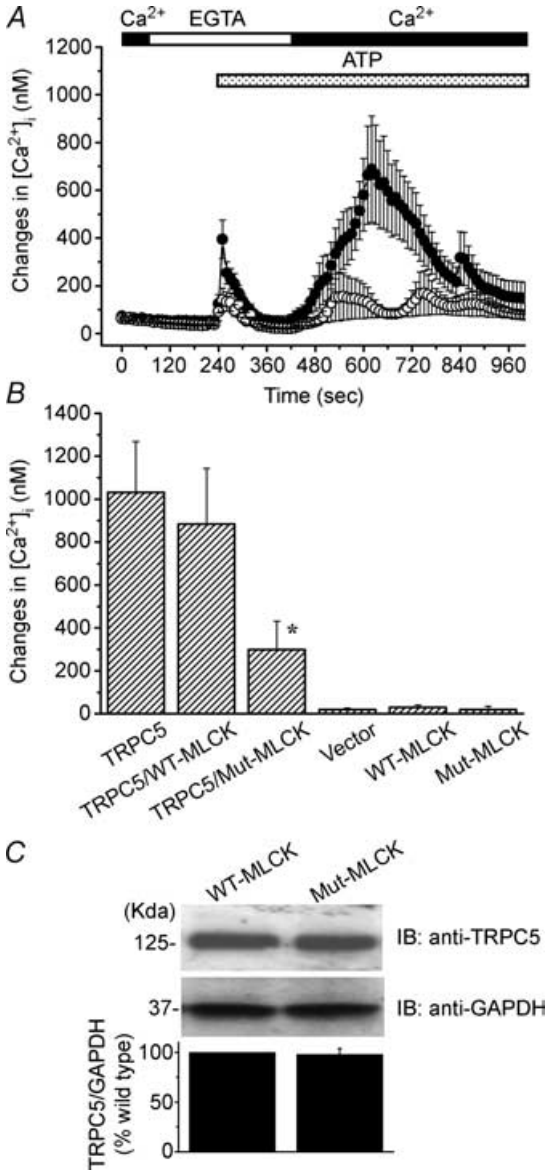

Figure 5. Suppression of TRPC5 channel activation by the dominant-negative mutant of MLCK (Mut-MLCK)
A, changes in $[Ca^{2+}]_i$ induced by ATP-receptor stimulation were compared between cells transfected with TRPC5 alone (●; $n = 18$) and cells transfected with TRPC5 plus Mut-MLCK (○; $n = 23$). The perfusion solution was first changed to Ca^{2+}-free HBS (shown as EGTA). Two minutes after the endogenous ATP receptor was stimulated by the application of 100 μM ATP to the cells in the absence of extracellular Ca^{2+}, 2 mM Ca^{2+} was applied to induce a rise in $[Ca^{2+}]_i$ due to Ca^{2+} entry via TRPC5 channels. *B*, the amplitude of maximum $[Ca^{2+}]_i$ rises induced by Ca^{2+} entry via TRPC5 channels in individual cells was shown for TRPC5 alone ($n = 18$), TRPC5 plus wild-type (WT)-MLCK ($n = 11$) and TRPC5 plus Mut-MLCK ($n = 23$). $[Ca^{2+}]_i$ rises via endogenous Ca^{2+} entry mechanism were also shown for vector ($n = 9$), WT-MLCK ($n = 7$) and Mut-MLCK ($n = 18$). $^*P < 0.05$ *versus* group expressing TRPC5 alone. *C*, the obtained protein (40 μg) from HEK293 cotransfected with TRPC5 plus WT-MLCK or plus Mut-MLCK was fractionated by SDS-PAGE, and immunoblotted with anti-TRPC5 antibody. The lower column shows the ratio density of TRPC5/GAPDH from three independent experiments.

activation of TRPC5 channels was inhibited by calmodulin inhibitors, suggesting that calmodulin plays an essential role in the activation of TRPC5 channels. This is supported by the observation that the ATP-induced inward current through TRPC5 channels was blocked by the replacement of extracellular Ca^{2+} by Ba^{2+}. The replacement of Ca^{2+} by Ba^{2+} may initially cause Ba^{2+} influx instead of Ca^{2+}, and

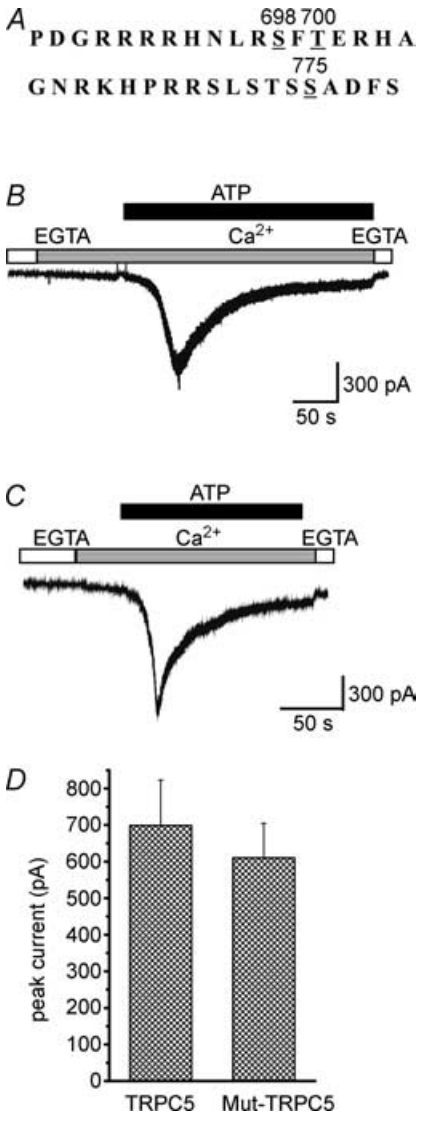

Figure 6. Effect of point mutation of putative phosphorylation sites in TRPC5 channels on ATP-evoked inward currents
A, amino-acid sequences containing possible phosphorylation sites. *B*, the ATP (100 μM)-evoked ionic current in the presence of 2 mM Ca^{2+} was measured in the wild-type TRPC5-expressing cell. *C*, three putative phosphorylation sites, S698, S775 and T700, by MLCK in the amino acid sequence of TRPC5 were point mutated to Ala, Ala and Val, respectively (a triple mutant S698A·S775A·T700V). The ATP (100 μM)-evoked ionic current in the presence of 2 mM Ca^{2+} was measured in the mutated TRPC5-expressing cell. *D*, the data show the peak current evoked by the addition of 100 μM ATP in wild-type and triple-mutated TRPC5-expressing HEK293 cells. Results are the means ± S.E.M. of $n = 4$ cells.

the accumulated Ba^{2+} may block the inward current by inhibition of the Ca^{2+}–calmodulin complex.

Implication of MLCK in the functional expression of TRPC5 channels

The ATP-receptor-induced activation of TRPC5 channels was further suppressed by inhibitors of MLCK, ML-9 and wortmannin. MLCK regulated by Ca^{2+}–calmodulin is believed to be a major kinase in both smooth muscle and non-muscle cells, and is potently inhibited by ML-9 through competition with ATP binding at the active centre of the kinase (Saitoh *et al.* 1987). ML-9 also 10-times weakly inhibits protein kinase C (PKC) and protein kinase A (PKA) (Saitoh *et al.* 1987). However, the inhibition of PKC and PKA is unlikely to be involved in the inhibition of TRPC5 channels by ML-9, because both PKC and PKA inhibitors failed to affect the ATP-induced activation of TRPC5 channels (unpublished results). Moreover, Venkatachalam *et al.* (2003) showed that PKC activation itself inhibits TRPC5 channel activity. Although wortmannin also inhibits PI3-kinase, the concentration range for the inhibition of PI3-kinase is much lower than that which inhibited Ca^{2+} influx via TRPC5 channels. Moreover, the ATP-induced activation of TRPC5 channels was not affected by LY294002, another inhibitor of PI3-kinase (data not shown). The hypothesis that the activation of TRPC5 channels is regulated by MLCK, is supported by our observation that co-expression of dominant-negative mutant MLCK inhibited the activation of TRPC5 channels. HEK293 cells used throughout the experiments indeed express the brain/EC-type of MLCK. Thus, our findings overall suggest that the Ca^{2+}–calmodulin-dependent MLCK pathway has an important role in regulation of the functional expression of TRPC5 channels. The observation that the basal level of phospho-MLC was decreased by the Ca^{2+} chelator BAPTA-AM also supports the above hypothesis.

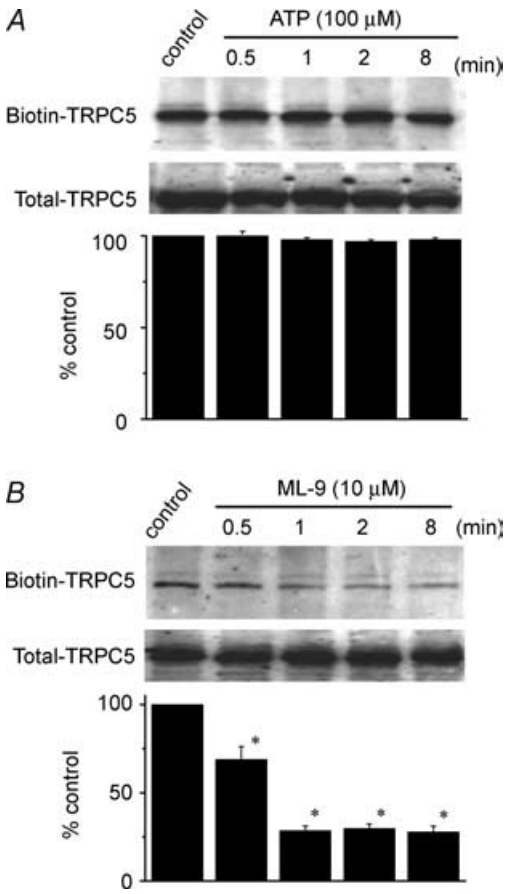

Figure 7. Impairment of cell surface expression of TRPC5 channels by MLCK inhibitor
The HEK293 cells transfected with TRPC5 were incubated with 100 μM ATP (*A*) or 10 μM ML-9 (*B*) for various period (0–8 min) and exposed to NHS-SS-biotin (Pirce). The cell lysates were then incubated with strepavidin-agarose (Pirce), and the obtained surface proteins were analysed by Western blot with an anti-TRPC5 antibody. To determine total amount of TRPC5, aliquots of cell lysates were taken before the incubation with strepavidin-agarose and analysed directly by Western blot. Each lower column shows the ratio density of biotin–TRPC5/total TRPC5 from three independent experiments. $^*P < 0.05$ *versus* control group.

Regulation of cell surface localization of TRPC5 channels by MLCK

Several hypotheses can be proposed to describe the mechanisms underlying the regulation of the functional expression of TRPC5 channels by MLCK. A favoured hypothesis is that phosphorylation of the MLC by MLCK underlies the activation of TRPC5 channels. As shown in Fig. 4, the inhibitor of MLCK reduced the basal level of phosphorylated MLC, whereas phosphorylation of MLC was not enhanced by ATP-receptor stimulation. Moreover, the MLCK inhibitor impaired the cell surface expression of TRPC5 protein in basal conditions. MLCK has been shown to change the cytoskeletal structure via phosphorylation of MLC in various types of cells (Kamm & Stull, 1985; Cai *et al.* 1998; Sanders *et al.* 1999). It is therefore possible that phosphorylation of MLC is essential for TRPC5 transportation to the plasma membrane, and the activity of MLCK under basal conditions is essential for the functional expression of TRPC5 channels at the plasma membrane. Once TRPC5 proteins are inserted into the plasma membrane, cellular signals such as G-proteins generated by receptor stimulation may trigger the opening of TRPC5 channels. This hypothesis is strongly supported by the observations that the basal single TRPC5 channel activity was suppressed by treatment with ML-9 in the whole-cell mode (Fig. 3*A* and *B*), but not in the inside-out mode (Fig. 3*C* and *D*). ML-9 is a cell-permeable substance that can diffuse across the plasma membrane (Ishikawa

et al. 1988) and reduce phospho-MLC levels (Fig. 4). In the whole-cell patch intact cells, the balance of MLC phosphorylation and dephosphorylation that regulates the plasma membrane localization of TRPC5 channels should remain intact and be susceptible to influence by ML-9. In the inside-out patch, which presumably lacks MLCK and MLC-phosphatase, TRPC5 channels already inserted in the plasma membrane should become independent of regulation by MLCK or inhibition by ML-9. In fact, localization of MLCK has been reported on stress fibres and in cleavage furrows (Guerriero *et al.* 1981; Totsukawa *et al.* 2000; Poperechnaya *et al.* 2000), and MLC-phosphatase has been shown to be present both within the cytoplasm and in the nucleus (Andreassen *et al.* 1998). It is important to note that the ineffectiveness of ML-9 on basal TRPC5 channel activity in the inside-out mode of patch clamp further excludes the possibility that ML-9 directly inhibit TRPC5 channels. It is interesting to note that recent studies have revealed activation of the store-operated channels by a conformational coupling mechanism between the plasma membrane and endoplasmic reticulum membrane (Kiselyov *et al.* 1998; Patterson *et al.* 1999), and block of the store-operated channel activation by displacement of actin (Ma *et al.* 2000). The cytoskeletal structure is primarily regulated by interactions of actin and myosin that are regulated by MLCK-mediated phosphorylation of the regulatory MLC (Wilmann *et al.* 2000). Our study, together with these previous studies, suggests that the interaction between actin and myosin by MLCK-mediated phosphorylation of MLC regulates plasma membrane localization of TRPC5 channels in store-independent activation as well.

Rapid TRPC5 channel internalization was revealed by inhibiting MLCK activity. After treatment for 1 min with 10 μM ML-9, TRPC5 currents were reduced to $53 \pm 4\%$ ($n = 30$; Fig. 2*G*), while phosphorylated MLC levels (Fig. 4*C*) and biotin–TRPC levels (Fig. 7*B*) were decreased to $61 \pm 7\%$ ($n = 3$) and $30 \pm 3\%$ ($n = 3$),

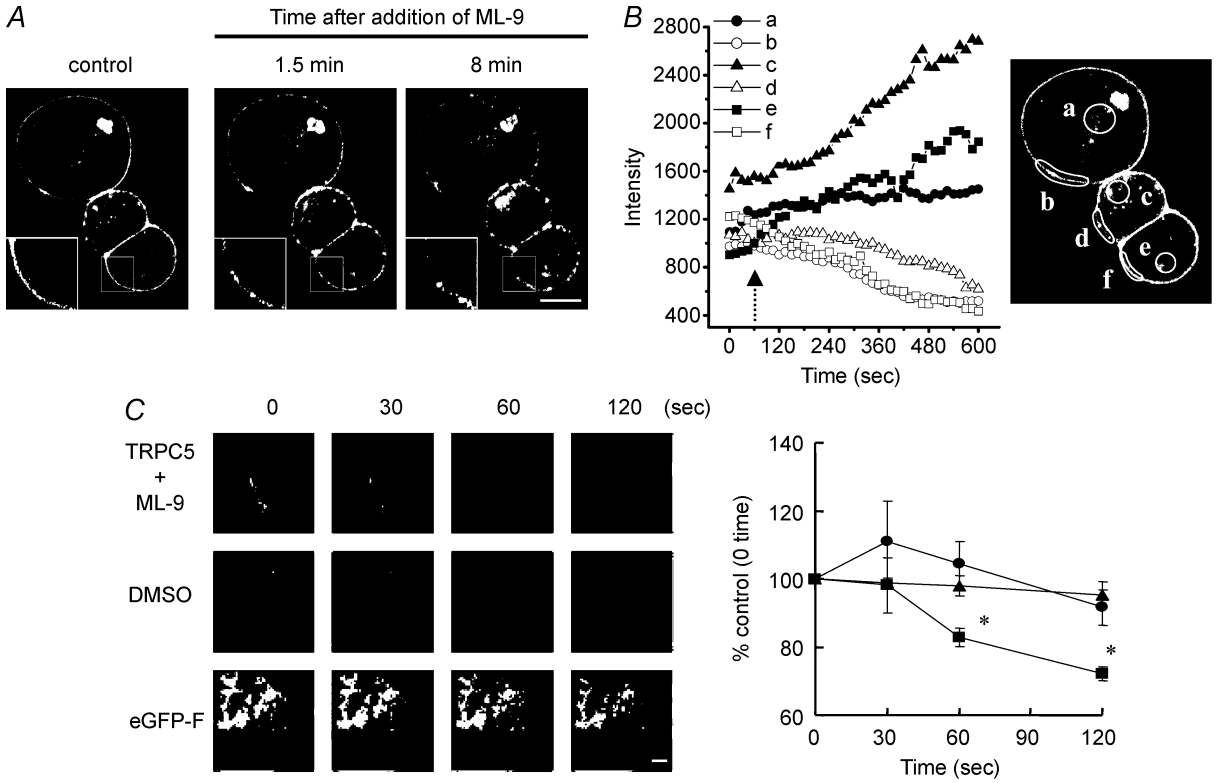

Figure 8. Effect of ML-9 on the cellular localization of TRPC5–eGFP fusion protein in a single HEK293 cell
A, image observed by confocal microscopy before (control) and after (1.5 and 8 min) stimulation with ML-9 (10 μM). Insets show a high magnification view of the boxed portion. Scale bar represents 10 μm. *B*, time course of the fluorescence intensity of TRPC5–eGFP measured in the indicated areas at the cytoplasm (a, c and e) and plasma membrane (b, d and f) is shown in the inset. The arrow indicates the time of ML-9 stimulation. A similar response was observed in 10 cells. *C*, left panel shows sequential images obtained by evanescent wave excitation in a single HEK293 cell expressing TRPC5–eGFP or eGFP-F observed before (0 s) and after stimulation (30, 60 and 120 s) with ML-9 or dimethyl sulphoxide. Scale bar represents 10 μm. Right panel shows time course of the fluorescence intensity change of TRPC5–eGFP (■) and eGFP-F (▲) stimulated with ML-9 (10 μM) or TRPC5–eGFP treated with dimethyl sulphoxide (●) measured in the whole part of a cell shown in the left panels. A similar response was observed in four cells. $^*P < 0.05$ *versus* control group.

respectively. Spontaneous TRPC5 channel activity showed more extensive reduction ($12 \pm 2\%$, $n = 6$; Fig. 3*B*), which can be attributed to the low concentration of Ca^{2+} (8 nM) in the external solution used for the measurement. It is conceivable that the TRPC5 channel insertion rapidly proceeds at the same high rate to counterbalance rapid internalization in maintaining a steady state of plasma membrane localization. Of interesting, rapid enhancement of surface expression via exocytotic insertion within 1–2 min upon growth factor stimulation has been demonstrated for recombinant and native neuronal TRPC5 channels as well as recombinant TRPC6 channels (Cayouette *et al.* 2004; Bezzerides *et al.* 2004). The time courses of trafficking of these channels were consistent with those in our observation for TRPC5. Regulation of channel function by exocytosis and endocytosis has been shown in various channels other than TRPC channels, including epithelial Na^+ channels, voltage-dependent Ca^{2+} channels, G-protein-gated K^+ channels, Ca^{2+}-activated K^+ channels, nicotinic acetylcholine receptors and cystic fibrosis transmembrane conductance regulator (CFTR) chloride channels (Carbonetto & Fambrough, 1979; Prince *et al.* 1994; Morishige *et al.* 1999; Snyder, 2000; Loffing *et al.* 2001; Viard *et al.* 2004; Chae & Dryer, 2005; Darsow *et al.* 2005; Gervasio & Phillips, 2005). The trafficking of exocrine epithelial CFTR chloride channels and endocrine G-protein-gated K^+ channels proceeded within 1 min, whereas that of epithelial Na^+ channels, neuronal Ca^{2+}-activated K^+ channels and nicotinic acetylcholine receptors in skeletal muscle and neurones was a much slower process and proceeded within > 1 h. The physiological significance of rapid trafficking of the TRPC5 channel and other channels is unknown. However, we can speculate that the activitiy of TRPC5 and other rapidly recycled ion channels are tightly linked to vesicle transport mechanisms responsible for exocytosis/endocytosis or for membrane recruitment at subcellular structures (Bezzerides *et al.* 2004). Extensive studies are needed to establish quantitative relationships between membrane dynamics and trafficking speeds of the TRPC5 channel in native systems.

Direct phosphorylation by MLCK is not involved in activation of TRPC5 channels

An alternative hypothesis is that MLCK directly phosphorylates TRPC5 protein to activate Ca^{2+} influx. However, this can be ruled out by the lack of influence of the point mutation of three potential phosphorylation sites on the activation of TRPC5-mediated Ca^{2+} influx. Moreover, although TRPC5 proteins from unstimulated and ATP-stimulated HEK293 cells were immunoprecipitated, and then immunoblotted by antiphosphoserine antibody and antiphosphothreonine antibody, the phosphorylated TRPC5 was not detected (data not shown). Finally, it is also possible that MLCK phosphorylates unknown regulatory proteins linked to the activation of TRPC5 channels. In-depth studies are necessary to understand how MLCK modulates plasma membrane localization of TRPC5 channels.

Roles of $[Ca^{2+}]_i$ in insertion and activation of TRPC5 channels

Considering our finding that stimulation of the ATP receptor failed to increase phosphorylation levels of MLC or cell surface expression of TRPC5 channels, maximal MLCK activation and TRPC5 protein insertion can be attained at basal $[Ca^{2+}]_i$. In TRPC5-expressing cells, slight but significant $[Ca^{2+}]_i$ reduction observed after omission of external Ca^{2+} (see Fig. 1*A*, *C* and *E*) suggests an $[Ca^{2+}]_i$ elevation by Ca^{2+} influx via spontaneously activated TRPC5 channels (Yamada *et al.* 2000). This may further support stabilization of maximal TRPC5 channel insertion. Therefore, the dramatic enhancement of Ca^{2+} influx upon ATP-receptor activation cannot involve additional TRPC5 protein insertion via the same MLCK pathway. However, maximal insertion of TRPC5 protein at resting $[Ca^{2+}]_i$ prior to ATP-receptor activation may poorly correlate with our explanation of how changing from Ca^{2+} to Ba^{2+} in the external solution induced a reduction in ATP-evoked currents through Ca^{2+}–calmodulin–MLCK-mediated insertion processes. The inconsistency may suggest that elevation of $[Ca^{2+}]_i$ upon ATP-receptor stimulation has effects independent of the Ca^{2+}–calmodulin–MLCK pathway. In this context, it is interesting to note that TRPC5 currents were elicited by intracellular infusion of solutions containing Ca^{2+} at higher concentrations ranging from 200 nM to 10 μM without G-protein activation (Schaefer *et al.* 2000; Zeng *et al.* 2004). Activation of IP_3-receptor, Ca^{2+}-release channels has also been reported to make an essential contribution to receptor-evoked TRPC5 currents (Kanki *et al.* 2001). Furthermore, with regard to direct action of Ca^{2+} and calmodulin, potential sites have been mapped in the primary structure of TRPC5 channels (Tang *et al.* 2001; Jung *et al.* 2003; Ordaz *et al.* 2005). Thus, multiple Ca^{2+} targets including calmodulin–MLCK, which mediates TRPC5 protein insertion to the plasma membrane, and G-proteins may form a 'signalsome' that controls fine-tuning of physiological TRPC5 channel activation.

Conclusion

In conclusion, our findings reveal an essential cascade in TRPC5 channel activation: the basal level of intracellular Ca^{2+} acts on calmodulin to activate MLCK, and the phosphorylation of MLC maintains cell surface localization of TRPC5 proteins. Thus, TRPC5 proteins

are constitutively expressed at the plasma membrane as channels activatable upon G-protein-coupled receptor stimulation.

References

Andreassen PR, Lacroix FB, Villa-Moruzzi E & Margolis RL (1998). Differential subcellular localization of protein phosphatase-1α, γ1, and δ isoforms during both interphase and mitosis in mammalian cells. *J Cell Biol* **141**, 1207–1215.

Aromolaran AS, Albert AP & Large WA (2000). Evidence for myosin light chain kinase mediating noradrenaline-evoked cation current in rabbit portal vein myocytes. *J Physiol* **524**, 853–863.

Berridge MJ (1993). Inositol trisphosphate and calcium signalling. *Nature* **361**, 315–325.

Berridge MJ (1995). Capacitative calcium entry. *Biochem J* **312**, 1–11.

Bezzerides VJ, Ramsey IS, Kotecha S, Greka A & Clapham DE (2004). Rapid vesicular translocation and insertion of TRP channels. *Nat Cell Biol* **6**, 709–720.

Birnbaumer L, Zhu X, Jiang M, Boulay G, Peyton M, Vannier B, Brown D, Platano D, Sadeghi H, Stefani E & Birnbaumer M (1996). On the molecular basis and regulation of cellular capacitative calcium entry: roles for Trp proteins. *Proc Natl Acad Sci U S A* **93**, 15195–15202.

Bootman MD & Berridge MJ (1995). The elemental principles of calcium signaling. *Cell* **83**, 675–678.

Boulay G (2002). Ca^{2+}-calmodulin regulates receptor-operated Ca^{2+} entry activity of TRPC6 in HEK-293 cells. *Cell Calcium* **32**, 201–207.

Boulay G, Zhu X, Peyton M, Jiang M, Hurst R, Stefani E & Birnbaumer L (1997). Cloning and expression of a novel mammalian homolog of Drosophila transient receptor potential (Trp) involved in calcium entry secondary to activation of receptors coupled by the Gq class of G protein. *J Biol Chem* **272**, 29672–29680.

Cai S, Pestic-Dragovich L, O'Donnell ME, Wang N, Ingber D, Elson E & de Lanerolle P (1998). Regulation of cytoskeletal mechanics and cell growth by myosin light chain phosphorylation. *Am J Physiol* **275**, C1349–C1356.

Carbonetto S & Fambrough DM (1979). Synthesis, insertion into the plasma membrane, and turnover of alpha-bungarotoxin receptors in chick sympathetic neurons. *J Cell Biol* **81**, 555–569.

Cayouette S, Lussier MP, Mathieu E, Bousquet SM & Boulay G (2004). Exocytotic insertion of TRPC6 channel into the plasma membrane upon Gq protein-coupled receptor activation. *J Biol Chem* **279**, 7241–7246.

Chae KS & Dryer SE (2005). The p38 mitogen-activated protein kinase pathway negatively regulates Ca^{2+}-activated K^+ channel trafficking in developing parasympathetic neurons. *J Neurochem* **94**, 367–379.

Clapham DE (1995). Calcium signaling. *Cell* **80**, 259–268.

Darsow T, Booker TK, Pina-Crespo JC & Heinemann SF (2005). Exocytic trafficking is required for nicotine-induced up-regulation of $\alpha_4\beta_2$ nicotinic acetylcholine receptors. *J Biol Chem* **280**, 18311–18320.

Fasolato C, Innocenti B & Pozzan T (1994). Receptor-activated Ca^{2+} influx: how many mechanisms for how many channels? *Trends Pharmacol Sci* **15**, 77–83.

Fein A, Payne R, Corson DW, Berridge MJ & Irvine RF (1984). Photoreceptor excitation and adaptation by inositol 1,4,5-trisphosphate. *Nature* **311**, 157–160.

Gervasio OL & Phillips WD (2005). Increased ratio of rapsyn to ACh receptor stabilizes postsynaptic receptors at the mouse neuromuscular synapse. *J Physiol* **562**, 673–685.

Gillette R & Green DJ (1983). Phenothiazines mimic the action of cAMP in potentiating slow inward current in a bursting molluscan neuron. *Brain Res* **273**, 384–386.

Guerriero V, Rowley DR & Means AR (1981). Production and characterization of an antibody to myosin light chain kinase and intracellular localization of the enzyme. *Cell* **27**, 449–458.

Hamill OP, Marty A, Neher E, Sakmann B & Sigworth FJ (1981). Improved patch-clamp techniques for high-resolution current recording from cells and cell-free membrane patches. *Pflugers Arch* **391**, 85–100.

Hanson PI & Schulman H (1992). Neuronal Ca^{2+}/calmodulin-dependent protein kinases. *Annu Rev Biochem* **61**, 559–601.

Hofmann T, Obukhov AG, Schaefer M, Harteneck C, Gudermann T & Schultz G (1999). Direct activation of human TRPC6 and TRPC3 channels by diacylglycerol. *Nature* **397**, 259–263.

Ishikawa T, Chijiwa T, Hagiwara M, Mamiya S, Saitoh M & Hidaka H (1988). ML-9 inhibits the vascular contraction via the inhibition of myosin light chain phosphorylation. *Mol Pharmacol* **33**, 598–603.

Jung S, Mühle A, Schaefer M, Strotmann R, Schultz G & Plant TD (2003). Lanthanides potentiate TRPC5 currents by an action at extracellular sites close to the pore mouth. *J Biol Chem* **278**, 3562–3571.

Jurman ME, Boland LM, Liu Y & Yellen G (1994). Visual identification of individual transfected cells for electrophysiology using antibody-coated beads. *Biotechniques* **17**, 876–881.

Kamm KE & Stull JT (1985). The function of myosin and myosin light chain kinase phosphorylation in smooth muscle. *Annu Rev Pharmacol Toxicol* **25**, 593–620.

Kamm KE & Stull JT (2001). Dedicated myosin light chain kinases with diverse cellular functions. *J Biol Chem* **276**, 4527–4530.

Kanki H, Kinoshita M, Akaike A, Satoh M, Mori Y & Kaneko S (2001). Activation of inositol 1,4,5-trisphosphate receptor is essential for the opening of mouse TRP5 channels. *Mol Pharmacol* **60**, 989–998.

Kemp BE, Pearson RB, Guerriero V Jr, Bagchi IC & Means AR (1987). The calmodulin binding domain of chicken smooth muscle myosin light chain kinase contains a pseudosubstrate sequence. *J Biol Chem* **262**, 2542–2548.

Kim YC, Kim SJ, Kang TM, Suh SH, So I & Kim KW (1997). Effects of myosin light chain kinase inhibitors on carbachol-activated nonselective cationic current in guinea-pig gastric myocytes. *Pflugers Arch* **434**, 346–353.

Kiselyov K, Xu X, Mozhayeva G, Kuo T, Pessah I, Mignery G, Zhu X, Birnbaumer L & Muallem S (1998). Functional interaction between InsP3 receptors and store-operated Htrp3 channels. *Nature* **396**, 478–482.

Klee CB & Vanaman TC (1982). Calmodulin. *Adv Protein Chem* **35**, 213–321.

Klemke RL, Cai S, Giannini AL, Gallagher PJ, de Lanerolle P & Cheresh DA (1997). Regulation of cell motility by mitogen-activated protein kinase. *J Cell Biol* **137**, 481–492.

Loffing J, Zecevic M, Féraille E, Kaissling B, Asher C, Rossier BC, Firestone GL, Pearce D & Verrey F (2001). Aldosterone induces rapid apical translocation of ENaC in early portion of renal collecting system: possible role of SGK. *Am J Physiol Renal Physiol* **280**, F675–F682.

Ma HT, Patterson RL, van Rossum DB, Birnbaumer L, Mikoshiba K & Gill DL (2000). Requirement of the inositol trisphosphate receptor for activation of store-operated Ca^{2+} channels. *Science* **287**, 1647–1651.

Morishige K, Inanobe A, Yoshimoto Y, Kurachi H, Murata Y, Tokunaga Y, Maeda T, Maruyama Y & Kurachi Y (1999). Secretagogue-induced exocytosis recruits G protein-gated K^+ channels to plasma membrane in endocrine cells. *J Biol Chem* **274**, 7969–7974.

Nairn AC & Picciotto MR (1994). Calcium/calmodulin-dependent protein kinases. *Semin Cancer Biol* **5**, 295–303.

Obukhov AG, Harteneck C, Zobel A, Harhammer R, Kalkbrenner F, Leopoldt D, Luckhoff A, Nurnberg B & Schultz G (1996). Direct activation of trpl cation channels by $G\alpha_{11}$ subunits. *EMBO J* **15**, 5833–5838.

Okada T, Inoue R, Yamazaki K, Maeda A, Kurosaki T, Yamakuni T, Tanaka I, Shimizu S, Ikenaka K, Imoto K & Mori Y (1999). Molecular and functional characterization of a novel mouse transient receptor potential protein homologue TRP7. *J Biol Chem* **274**, 27359–27370.

Okada T, Shimizu S, Wakamori M, Maeda A, Kurosaki T, Takada N, Imoto K & Mori Y (1998). Molecular cloning and functional characterization of a novel receptor-activated TRP Ca^{2+} channel from mouse brain. *J Biol Chem* **273**, 10279–10287.

Ordaz B, Tang J, Xiao R, Salgado A, Sampieri A, Zhu MX & Vaca L (2005). Calmodulin and calcium interplay in the modulation of TRPC5 channel activity. *J Biol Chem* **280**, 30788–30796.

Patterson RL, van Rossum DB & Gill DL (1999). Store-operated Ca^{2+} entry: evidence for a secretion-like coupling model. *Cell* **98**, 487–499.

Petersen CCH, Berridge MJ, Borgese MF & Bennett DL (1995). Putative capacitative calcium entry channels: expression of Drosophila trp and evidence for the existence of vertebrate homologues. *Biochem J* **311**, 41–44.

Philipp S, Cavalié A, Freichel M, Wissenbach U, Zimmer S, Trost C, Marquart A, Murakami M & Flockerzi V (1996). A mammalian capacitative calcium entry channel homologous to Drosophila TRP and TRPL. *EMBO J* **15**, 6166–6171.

Philipp S, Hambrecht J, Braslavski L, Schroth G, Freichel M, Murakami M, Cavalié A & Flockerzi V (1998). A novel capacitative calcium entry channel expressed in excitable cells. *EMBO J* **17**, 4274–4282.

Poperechnaya A, Varlamova O, Lin PJ, Stull JT & Bresnick AR (2000). Localization and activity of myosin light chain kinase isoforms during the cell cycle. *J Cell Biol* **151**, 697–708.

Prince LS, Workman RB & Marchase RB (1994). Rapid endocytosis of the cystic fibrosis transmembrane conductance regulator chloride channel. *Proc Natl Acad Sci U S A* **91**, 5192–5196.

Putney JW Jr (1990). Capacitative calcium entry revisited. *Cell Calcium* **11**, 611–624.

Ranganathan R, Malicki DM & Zuker CS (1995). Signal transduction in Drosophila photoreceptors. *Annu Rev Neurosci* **18**, 283–317.

Saitoh M, Ishikawa T, Matsushima S, Naka M & Hidaka H (1987). Selective inhibition of catalytic activity of smooth muscle myosin light chain kinase. *J Biol Chem* **262**, 7796–7801.

Sakurada K, Seto M & Sasaki Y (1998). Dynamics of myosin light chain phosphorylation at Ser19 and Thr18/Ser19 in smooth muscle cells in culture. *Am J Physiol* **274**, C1563–C1572.

Sanders LC, Matsumura F, Bokoch GM & de Lanerolle P (1999). Inhibition of myosin light chain kinase by p21-activated kinase. *Science* **283**, 2083–2085.

Schaefer M, Plant TD, Obukhov AG, Hofmann T, Gudermann T & Schultz G (2000). Receptor-mediated regulation of the nonselective cation channels TRPC4 and TRPC5. *J Biol Chem* **275**, 17517–17526.

Singh BB, Liu X, Tang J, Zhu MX & Ambudkar IS (2002). Calmodulin regulates Ca^{2+}-dependent feedback inhibition of store-operated Ca^{2+} influx by interaction with a site in the C terminus of TRPC1. *Mol Cell* **9**, 739–750.

Snyder PM (2000). Liddle's syndrome mutations disrupt cAMP-mediated translocation of the epithelial Na^+ channel to the cell surface. *J Clin Invest* **105**, 45–53.

Strübing C, Krapivinsky G, Krapivinsky L & Clapham DE (2001). TRPC1 and TRPC5 form a novel cation channel in mammalian brain. *Neuron* **29**, 645–655.

Tang J, Lin Y, Zhang Z, Tikunova S, Birnbaumer L & Zhu MX (2001). Identification of common binding sites for calmodulin and inositol 1, 4, 5-trisphosphate receptors on the carboxyl termini of Trp channels. *J Biol Chem* **276**, 21303–21310.

Totsukawa G, Yamakita Y, Yamashiro S, Hartshorne DJ, Sasaki Y & Matsumura F (2000). Distinct roles of ROCK (Rho-kinase) and MLCK in spatial regulation of MLC phosphorylation for assembly of stress fibers and focal adhesions in 3T3 fibroblasts. *J Cell Biol* **150**, 797–806.

Tran QK, Watanabe H, Zhang XX, Takahashi R & Ohno R (1999). Involvement of myosin light chain kinase in chloride-sensitive Ca^{2+} influx in porcine aortic endothelial cells. *Cardiovasc Res* **44**, 623–631.

Trost C, Bergs C, Himmerkus N & Flockerzi V (2001). The transient receptor potential, TRP4, cation channel is a novel member of the family of calmodulin binding proteins. *Biochem J* **355**, 663–670.

Ueda S & Okada Y (1989). Acid secretagogues induce Ca^{2+} mobilization coupled to K^+ conductance activation in rat parietal cells in tissue culture. *Biochim Biophys Acta* **1012**, 254–260.

Venkatachalam K, Zheng F & Gill DL (2003). Regulation of canonical transient receptor potential (TRPC) channel function by diacylglycerol and protein kinase C. *J Biol Chem* **278**, 29031–29040.

Viard P, Butcher AJ, Halet G, Davies A, Nürnberg B, Heblich F & Dolphin AC (2004). PI3K promotes voltage-dependent calcium channel trafficking to the plasma membrane. *Nat Neurosci* **7**, 939–946.

Watanabe H, Takahashi R, Zhang XX, Goto Y, Hayashi H, Ando J, Isshiki M, Seto M, Hidaka H, Niki I & Ohno R (1998). An essential role of myosin light-chain kinase in the regulation of agonist- and fluid flow-stimulated Ca^{2+} influx in endothelial cells. *FASEB J* **12**, 341–348.

Wes PD, Chevesich J, Jeromin A, Rosenberg C, Stetten G & Montell C (1995). TRPC1, a human homolog of Drosophila store-operated channel. *Proc Natl Acad Sci U S A* **92**, 9652–9656.

Wilmann M, Gautel M & Mayans O (2000). Activation of calmodulin regulated kinases. *Cell Mol Biol* **46**, 883–894.

Xu XZ, Li HS, Guggino WB & Montell C (1997). Coassembly of TRP and TRPL produces a distinct store-operated conductance. *Cell* **89**, 1155–1164.

Yamada H, Wakamori M, Hara Y, Takahashi Y, Konishi K, Imoto K & Mori Y (2000). Spontaneous single-channel activity of neuronal TRP5 channel recombinantly expressed in HEK293 cells. *Neurosci Lett* **285**, 111–114.

Zeng F, Xu SZ, Jackson PK, McHugh D, Kumar B, Fountain SJ & Beech DJ (2004). Human TRPC5 channel activated by a multiplicity of signals in a single cell. *J Physiol* **559**, 739–750.

Zhang Z, Tang J, Tikunova S, Johnson JD, Chen Z, Qin N, Dietrich A, Stefani E, Birnbaumer L & Zhu MX (2001). Activation of TRP3 by inositol 1,4,5-triphosphate receptors through displacement of inhibitory calmodulin from a common binding domain. *Proc Natl Acad Sci U S A* **98**, 3168–3173.

Zhu X, Jiang M & Birnbaumer L (1998). Receptor-activated Ca^{2+} influx via human Trp3 stably expressed in human embryonic kidney (HEK) 293 cells. Evidence for a non-capacitative Ca^{2+} entry. *J Biol Chem* **273**, 133–142.

Zhu X, Jiang M, Peyton M, Boulay G, Hurst R, Stefani E & Birnbaumer L (1996). trp, a novel mammalian gene family essential for agonist-activated capacitative Ca^{2+} entry. *Cell* **85**, 661–671.

Zitt C, Obukhov AG, Strübing C, Zobel A, Kalkbrenner F, Lückhoff A & Schultz G (1997). Expression of TRPC3 in Chinese hamster ovary cells results in calcium-activated cation currents not related to store depletion. *J Cell Biol* **138**, 1333–1341.

Zitt C, Zobel A, Obukhov AG, Harteneck C, Kalkbrenner F, Lückhoff A & Schultz G (1996). Cloning and functional expression of a human Ca^{2+}-permeable cation channel activated by calcium store depletion. *Neuron* **16**, 1189–1196.

Acknowledgements

We thank Keiji Imoto for helpful discussion, and Emiko Mori, Hisanobu Yamada and Kumiko Saito for expert technical assistance.